

AD-A173 323

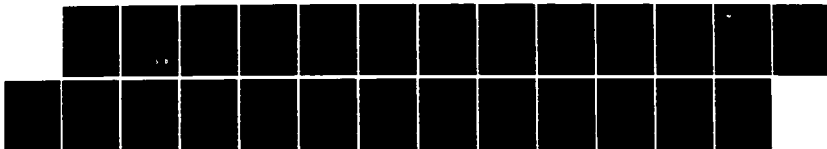
METALLIC INDUCTION REACTION ENGINE(U) ELECTROMAGNETIC  
LAUNCH RESEARCH INC CAMBRIDGE MA D HART ET AL.  
27 NOV 85 EML-85-AF002 AFOSR-TR-86-0933

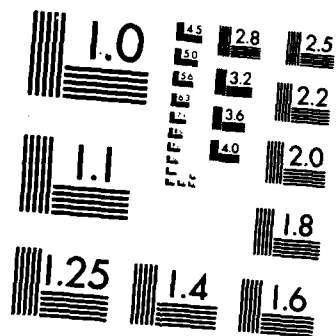
1/1

UNCLASSIFIED

F/G 21/3

NL





MICROCOPY RESOLUTION TEST CHART  
NATIONAL BUREAU OF STANDARDS-1963-A

(2)

AFOSR-TR- 86-0938

**METALLIC INDUCTION REACTION ENGINE**AFOSR Final Report  
Contract F49620-84-C-0093Douglas Hart, M.S.  
Peter P. Mongeau, Ph.D.  
Henry H. Kolm, Ph.D.Electromagnetic Launch Research, Inc.  
Cambridge, MA 02139Approved for public release;  
distribution unlimited.**ABSTRACT**

Metal rings placed close to a pulsed field coil have been accelerated at 200 million gee to 5 km/s in a 2 cm length by Bandoletov in the USSR [Bandoletov, 1977]. We have studied the basic phenomena and ultimate limitations of the pulsed induction process both theoretically and experimentally to determine its usefulness as a reaction engine. It is possible in principle to accelerate metal rings at high efficiency, and impart sufficient energy to ensure melting and evaporation, so that the reaction mass is ultimately ejected in the form of plasma. In practice, the process is limited by electrical, mechanical and thermal failure of the induction coil. Over a hundred shots were fired, including several in which 12 gram rings were accelerated to over 700 m/s at efficiencies above 30 percent. This is equivalent to the performance of a high power rifle with a one inch long barrel. An unexpected result of these studies is the discovery that to achieve maximum velocity, the mutual inductance gradient between induction coil and projectile ring in the firing position must be reduced to minimize the initial acceleration. This reduces the back-voltage and increases the interaction time, resulting in maximum energy transfer.

AIR FORCE OFFICE OF SCIENTIFIC RESEARCH (AFSC)  
NOTICE OF TRANSMITTAL TO DTICThis technical report has been reviewed and is  
approved for public release IAW AFR 190-12.

Distribution is unlimited.

ATTENTION: DTIC

Chief, Technical Information Division

DTIC  
ELECTE  
S OCT 20 1986 D  
D

DTIC FILE COPY

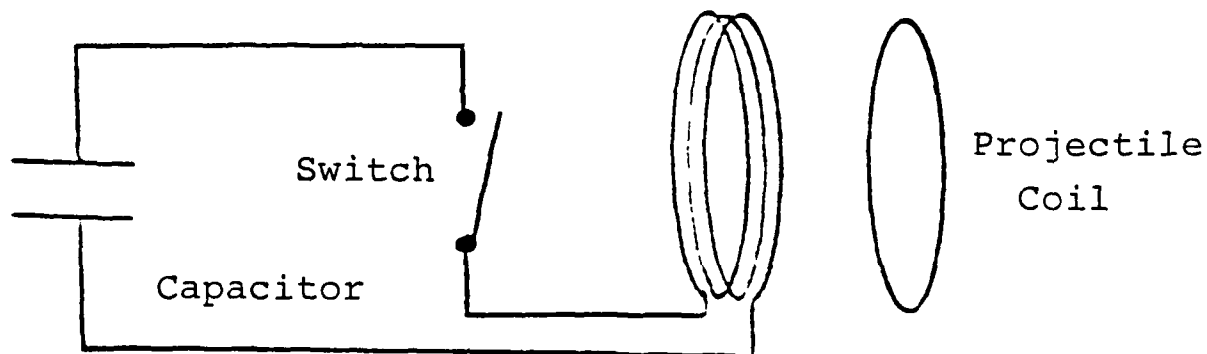
# REPORT DOCUMENTATION PAGE

|   |       |  |  |   |   |
|---|-------|--|--|---|---|
| 1a. REPORT SECURITY CLASSIFICATION<br><b>UNCLASSIFIED</b>   |       |  | 1b. RESTRICTIVE MARKINGS   |   |   |
| 2a. SECURITY CLASSIFICATION AUTHORITY   |       |  | 3. DISTRIBUTION/AVAILABILITY OF REPORT<br><del>Approved for public release,<br/>Distribution unlimited</del> |   |   |
| 2b. DECLASSIFICATION/DOWNGRADING SCHEDULE   |       |  | 4. PERFORMING ORGANIZATION REPORT NUMBER(S)<br><b>EML-85-AF002</b>   |   |   |
| 5. MONITORING ORGANIZATION REPORT NUMBER(S)<br><b>AFOSR-TR-86-0988</b>  |       |  | 6a. NAME OF PERFORMING ORGANIZATION<br>Electromagnetic Launch<br>Research, Inc.                              |   |   |
| 6b. OFFICE SYMBOL<br>(If applicable)<br><b>NA</b>   |       |  | 7a. NAME OF MONITORING ORGANIZATION<br>Air Force Office of Scientific Research                               |   |   |
| 6c. ADDRESS (City, State and ZIP Code)<br>625 Putnam Avenue<br>Cambridge, Massachusetts 02139   |       |  | 7b. ADDRESS (City, State and ZIP Code)<br>Building 410<br>Bolling AFB, Washington D.C. 20332-6448            |   |   |
| 8a. NAME OF FUNDING/SPONSORING ORGANIZATION<br><b>AFOSR</b>   |       |  | 8b. OFFICE SYMBOL<br>(If applicable)<br><b>NA</b>  |   |   |
| 8c. ADDRESS (City, State and ZIP Code)<br><b>Bolling AFB DC 20332-6448</b>  |       |  | 9. PROCUREMENT INSTRUMENT IDENTIFICATION NUMBER<br>F49620-84-C-0093  |   |   |
| 11. TITLE (Include Security Classification)<br>Metallic Induction Reaction Engine   |       |  | 10. SOURCE OF FUNDING NOS.   |   |   |
|   |       |  | PROGRAM ELEMENT NO. PROJECT NO. TASK NO. WORK UNIT NO.   |   |   |
|   |       |  | <b>61102F 2308 A1</b>  |   |   |
| 12. PERSONAL AUTHOR(S)<br>Hart, Douglas P., Mongeau, Peter P., Kolm, Henry H.   |       |  |  |   |   |
| 13a. TYPE OF REPORT<br>FINAL  |       | 13b. TIME COVERED<br>FROM 15AUG84 TO 14AUG85 |  | 14. DATE OF REPORT (Yr., Mo., Day)<br>85NOV27 |   |
| 15. PAGE COUNT<br>23  |       |  |  |   |   |
| 16. SUPPLEMENTARY NOTATION  |       |  |  |   |   |
| 17. COSATI CODES  |       |  | 18. SUBJECT TERMS (Continue on reverse if necessary and identify by block number)                            |   |   |
| FIELD   | GROUP | SUB. GR.                                     | Electric Propulsion, Pulse Coil, Pulsed Power, Accelerator   |   |   |
| 21  | 03    |  |  |   |   |
| 19. ABSTRACT (Continue on reverse if necessary and identify by block number)  |       |  |  |   |   |
| <p>Metal rings placed close to a pulsed field coil have been accelerated at 200 million gee to 5km/s in a 2cm length by Bandoletov in the USSR (Bandoletov, 1977). We have studied the basic phenomena and ultimate limitations of the pulsed induction process both theoretically and experimentally to determine its usefulness as a reaction engine. It is possible in principle to accelerate metal rings at high efficiency, and impart sufficient energy to ensure melting and evaporation, so that the reaction mass is ultimately ejected in the form of plasma. In practice, the process is limited by electrical, mechanical and thermal failure of the induction coil. Over a hundred shots were fired, including several in which 12 gram rings were accelerated to over 700 m/s at efficiencies above 30 percent. This is equivalent to the performance of a high power rifle with a one inch long barrel. An unexpected result of these studies is the discovery that to achieve maxium velocity, the mutual inductance gradient between induction coil and projectile ring in the firing position must be reduced to minimize the initial acceleration. This reduces the back-voltage and increases the interaction time, resulting in maxium energy transfer.</p> |       |  |  |   |   |
| 20. DISTRIBUTION/AVAILABILITY OF ABSTRACT<br>UNCLASSIFIED/UNLIMITED <input checked="" type="checkbox"/> SAME AS RPT. <input type="checkbox"/> DTIC USERS <input type="checkbox"/>   |       |  | 21. ABSTRACT SECURITY CLASSIFICATION<br>UNCLASSIFIED   |   |   |
| 22a. NAME OF RESPONSIBLE INDIVIDUAL<br>Dr. Leonard Caveny   |       |  | 22b. TELEPHONE NUMBER<br>(Include Area Code)<br>202 767-4987   |   | 22c. OFFICE SYMBOL<br>AFOSR<br>Aerospace Sciences |

### INTRODUCTION

Advances in electrical propulsion have inspired a variety of approaches for orbit raising propulsion. One such technique, the metallic induction reaction engine, uses a solid metallic reaction mass rather than a gas or plasma to achieve high thrust density and efficiency. The reaction mass is inductively accelerated by a magnetic pulse coil, thereby eliminating the problems of erosion and wear. Conceptually this thruster is very similar to an inductive argon thruster except that a highly conductive metal is used as the reaction mass rather than an ionized gas [Hart, 1985]. Like the argon thruster, a ring is formed from the reaction mass and placed in close proximity to a magnetic pulse coil. Current flowing in the coil magnetically induces an opposing current in the reaction mass ring. The magnetic fields generated by these two currents interact to produce a force which accelerates the ring away from the pulse coil thereby producing thrust (see figure 1.).

Fig. 1: Reaction Engine Schematic.



Drive  
Coil



|                    |                                     |
|--------------------|-------------------------------------|
| Accession For      |                                     |
| NTIS CRA&I         | <input checked="" type="checkbox"/> |
| DTIC TAB           | <input type="checkbox"/>            |
| Unannounced        | <input type="checkbox"/>            |
| Justification      |                                     |
| By                 |                                     |
| Distribution/      |                                     |
| Availability Codes |                                     |
| Dist               | Avail and/or Special                |
| A-1                |                                     |

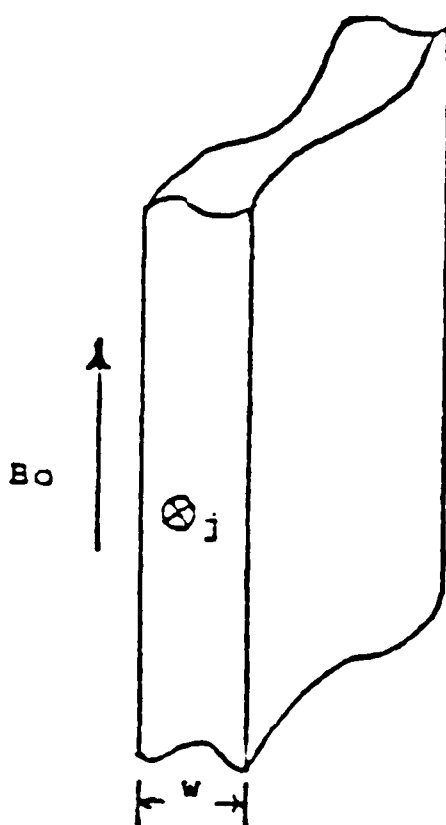
Although the fundamental operating principles of the metallic induction reaction engine have been previously established, little was known about the basic operating mechanisms and limitations of this device [Mongeau 1981]. During the past three years, Electromagnetic Launch Research, Inc. has been investigating the pulsed induction acceleration process. It was the goal of this research to establish the basic energy transfer mechanisms and the performance limitations of this device.

### RESEARCH SUMMARY

Research into the physics of the metallic induction reaction engine was approached from both a theoretical and experimental perspective.

Theoretical analysis of the engine is difficult because of the highly interdependent relationships between the parameters of the equations governing inductive energy transfer. In an attempt to alleviate this difficulty, a simple constant magnetic field model was developed. This model is based on a thin current carrying conductor of width  $w$  accelerated by a magnetic field  $B_0$  (see figure 2).

Fig 2. Ideal Model



The equations governing this model are;

$$W \rho \frac{J^2 z}{J+1} = \frac{B_0^2}{2 \mu_0} \quad (1)$$

and

$$B_0 = \mu_0 J W \quad (2)$$

If the conductor is assumed to accelerate a distance  $z$ , then the total kinetic energy imparted to the conductor per unit surface area is;

$$\frac{1}{2} \rho W z^2 = \frac{B_0^2 z}{2 \mu_0} \quad (3)$$

and the velocity is:

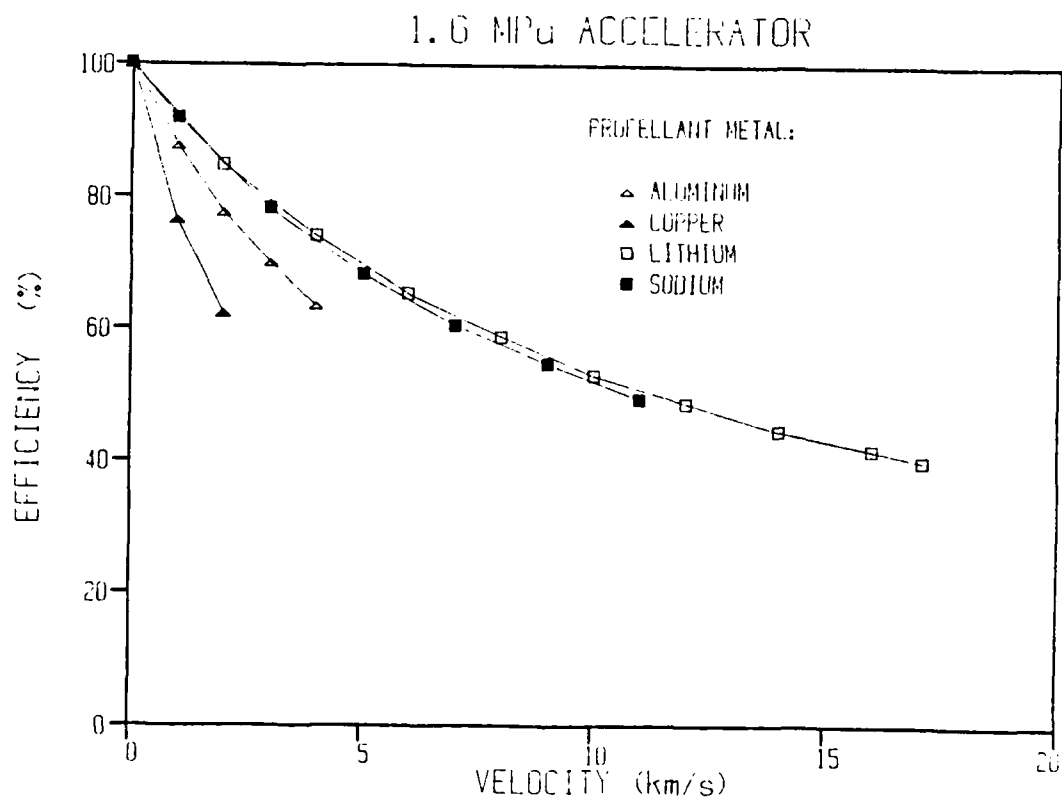
$$V = \left[ \frac{B_0^2 z J}{2 \rho J+1} \right]^{1/3}, \quad J = \int_0^z J dz \quad (4)$$

and the efficiency of this acceleration is:

$$\eta = Q B_0^2 z / (Q B_0^2 z + \rho V) \quad (5)$$

where  $Q$  is the conductivity of the conductor. When equation (5) is plotted as a function of velocity for several materials, it can be seen that low density materials such as lithium and sodium perform considerably better than highly conductive but relatively dense materials such as copper (see figure 3).

Fig 3. Ideal Performance Comparison



Although this model provides a useful comparison between the basic material and magnetic parameters, it does not account for effects such as the variations in magnetic coupling with separation, and temperature dependent resistivity that exist in a practical pulsed induction accelerator. Because of this, it is necessary to solve the complete set of governing equations including electrodynamic, thermodynamic, and magnetic coupling effects. Fortunately there exist several excellent numerical techniques which can be used to find accurate solutions. The effort needed to implement these numerical methods is greatly reduced by rewriting the governing equations in terms of magnetic flux. This results in the following set of equations;

and

These equations are easily solved using the Euler forward method. Although this is only a first order finite difference scheme, it provides sufficient accuracy and stability for studying basic parametric relationships. Using a similar technique, the detailed effects of ohmic heating, nonlinear material behavior, and magnetic coupling can be introduced into the solution. The result is a numerical model which has proven to be accurate to within 15% of experimental results over a broad range of testing conditions. Typical results of this model are shown in figure 4.

Observations and direct measurements of the pulsed induction acceleration process were made using an experimental apparatus consisting of an 18" diameter glass vacuum vessel sealed between aluminum and G-10 end plates. The aluminum end plate supports a plexiglass viewing port and the G-10 plate is built to allow various pulse coil designs to be easily mounted for testing (see figure 5).

Projectile acceleration was achieved by placing the projectile ring on the pulse coil, pumping down the vacuum chamber pressure, and discharging an 18 kilojoule capacitor bank through a dielectric switch into the pulse coil. Measurements of capacitor voltage, pulse coil current, and projectile ring position were made as well as photographic observations of the projectile ring in flight (see figures 6,7, and 8).



Fig 4: Typical Numerical Results

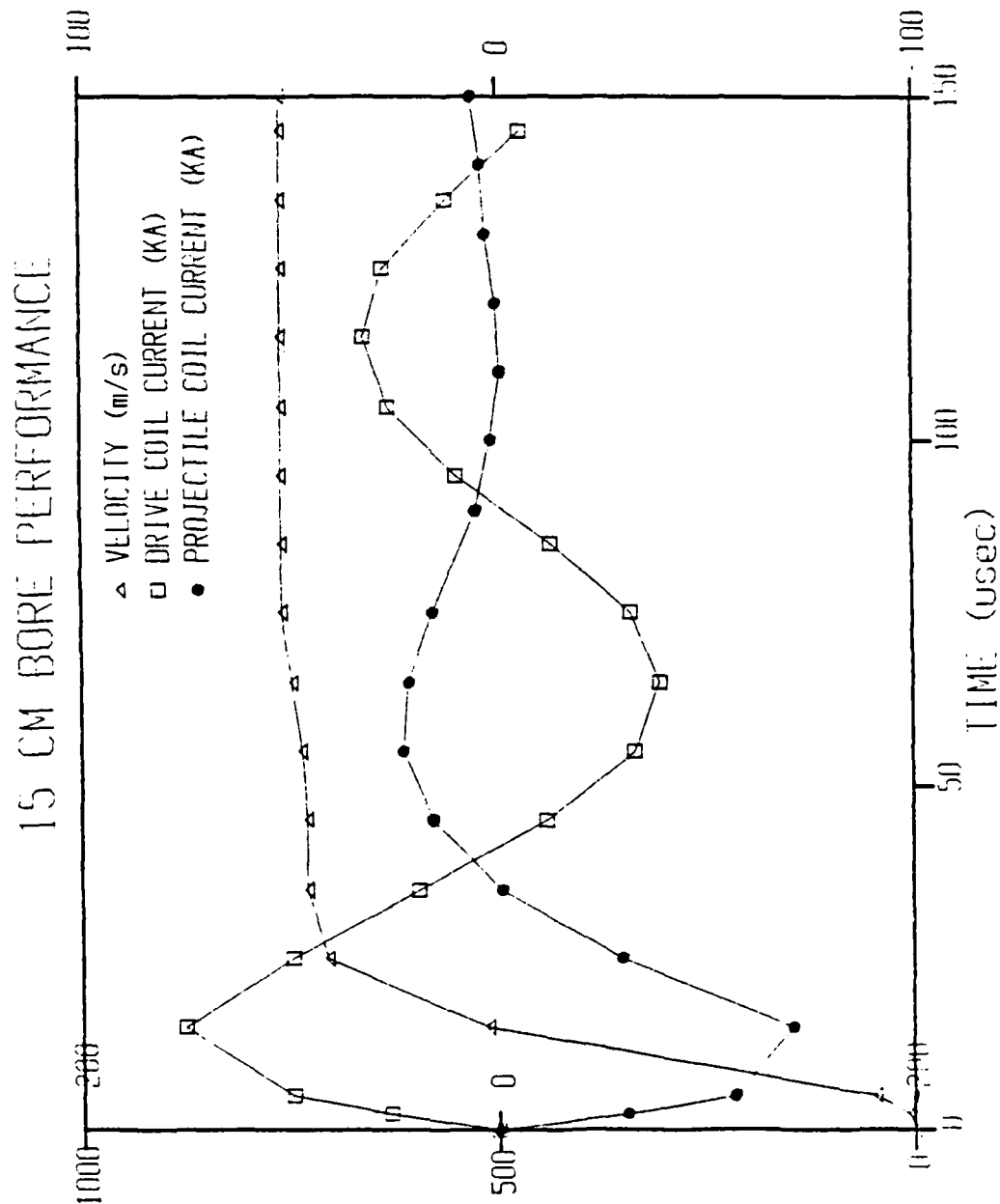


Fig. 5: Experimental Setup

Pulsed Induction Experimental Setup  
(Cross-Sectional View)

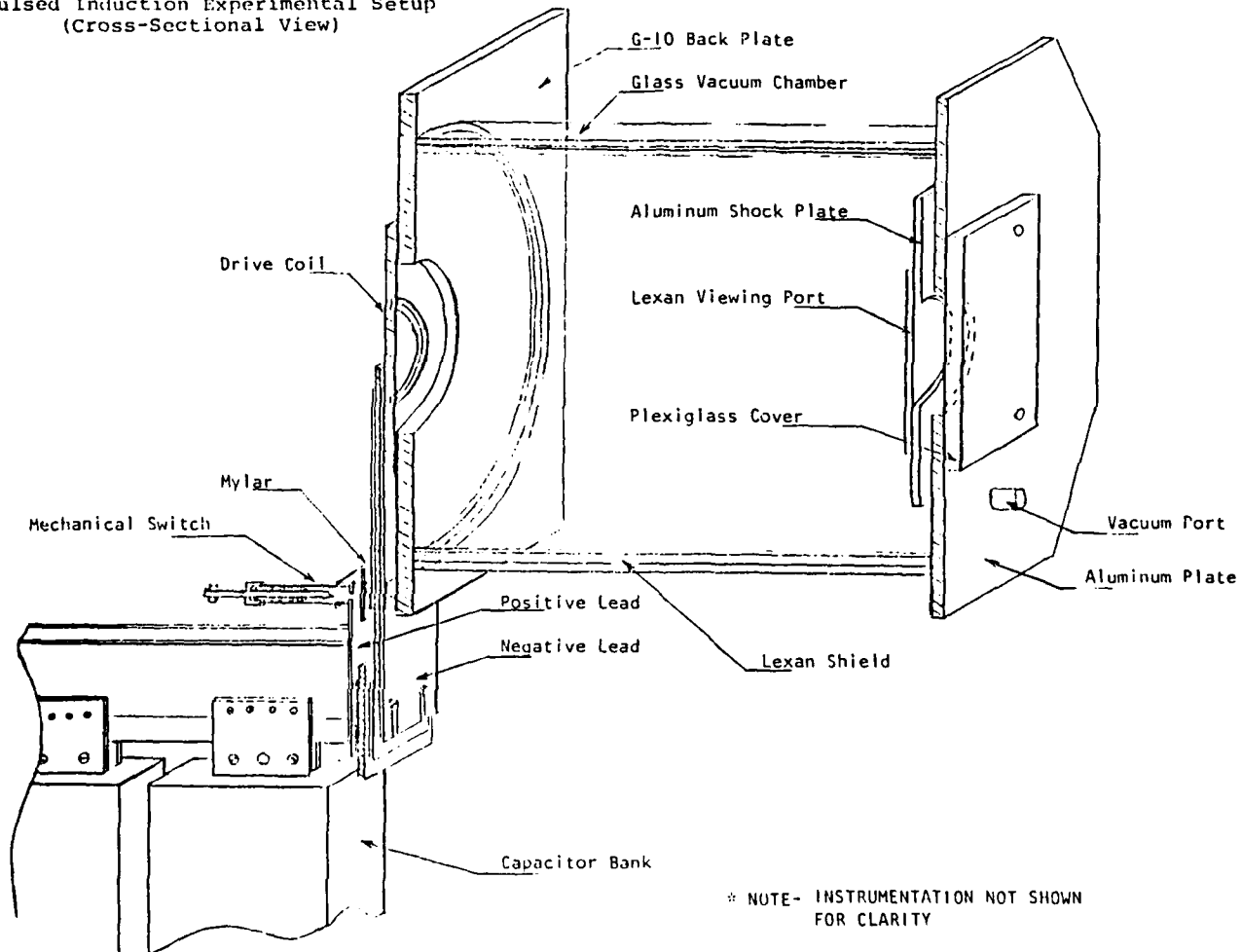


Fig. 6: Typical Voltage and Current Traces.

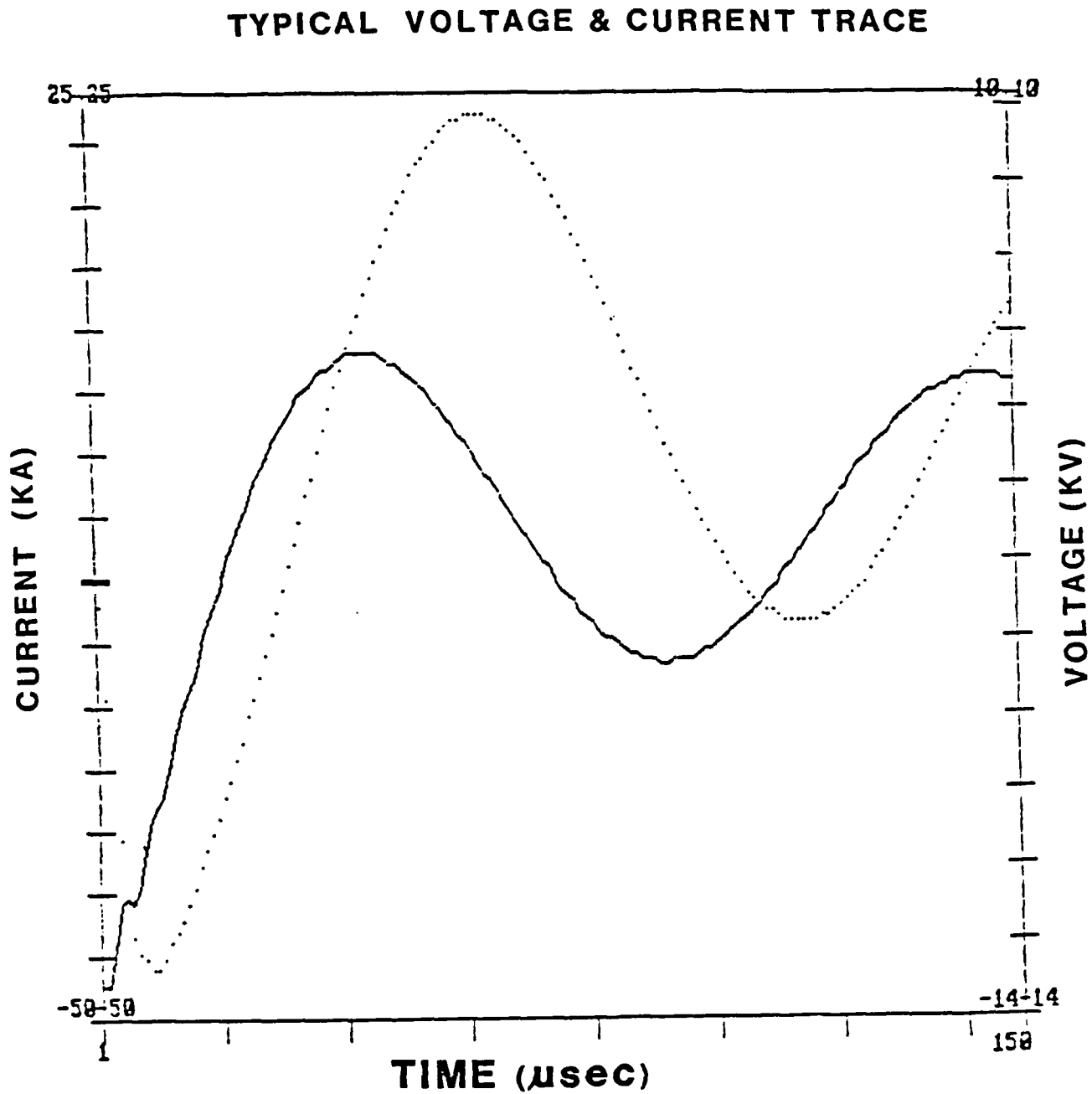


Fig. 7: Typical Laser Velocity Trace.

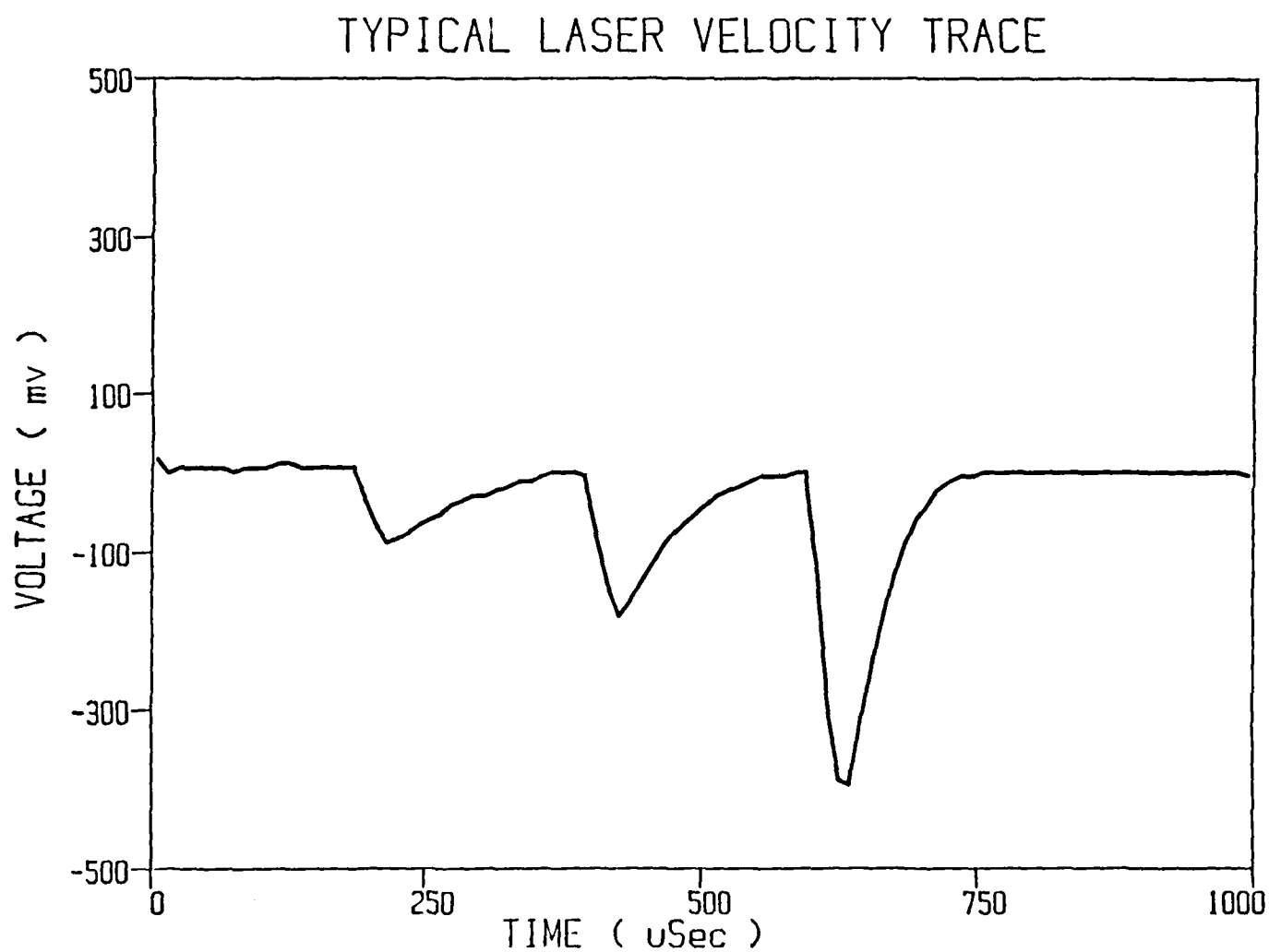
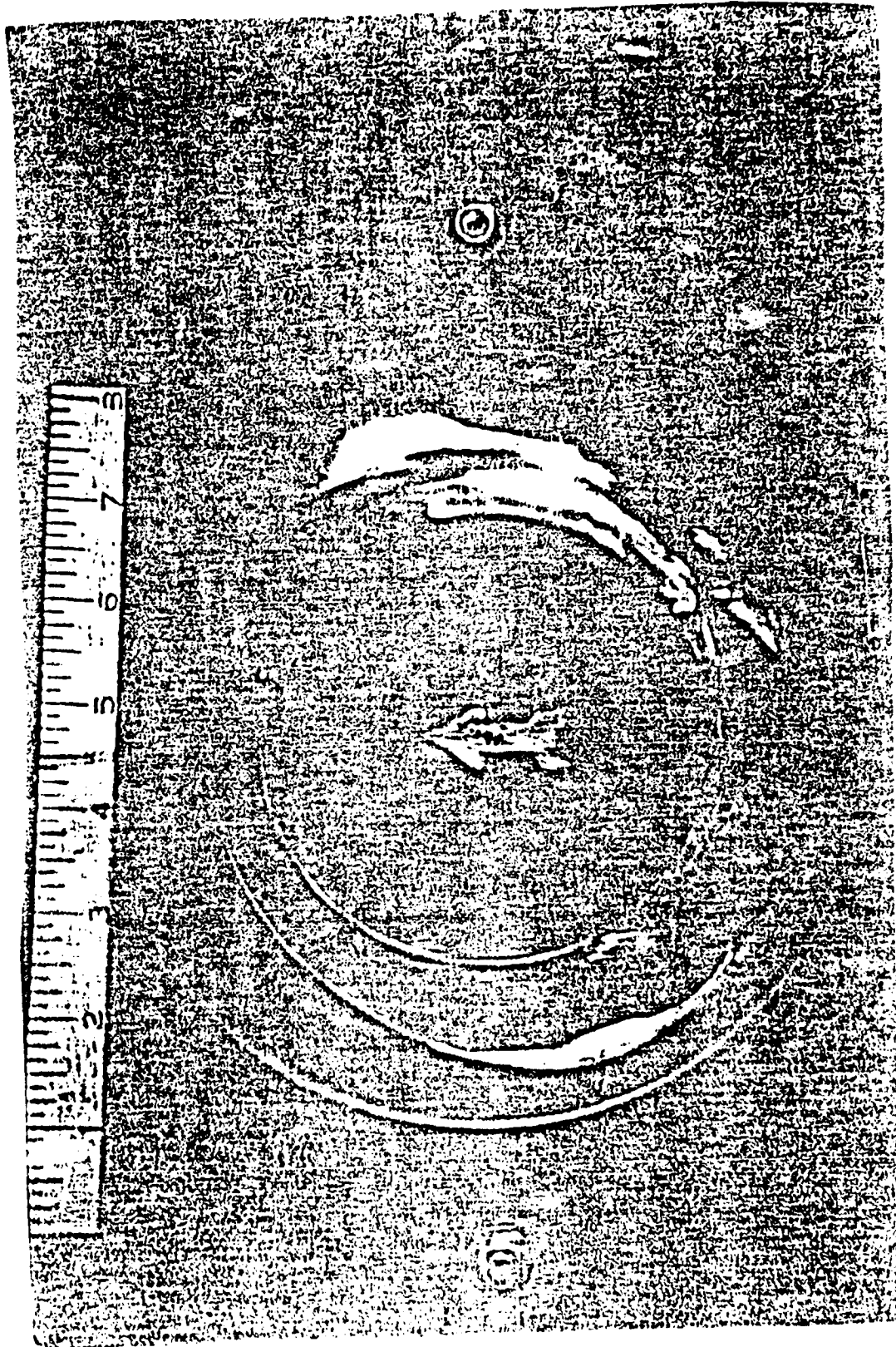


Fig. 8 Aluminum Reaction Mass Ring in Flight at 750 m/s.



Over one hundred tests using aluminum and copper reaction mass materials were performed with this apparatus including several tests with conversion efficiencies greater than 50 percent and velocities in excess of 700 meters per second (the experimental data is listed in appendix I.)

### PERFORMANCE CONSIDERATIONS

Optimizing the performance of the metallic induction reaction engine is difficult because of the large number of magnetic, geometric, and material properties involved. Although the exact relationships between the different parameters cannot be easily described, the general effect of each can.

The most fundamental parameters of the metallic induction reaction engine are the magnetic coupling parameters. These include the self inductance and mutual inductance of the two coils. From these parameters, the maximum ideal operating efficiency of this type of engine can be found;

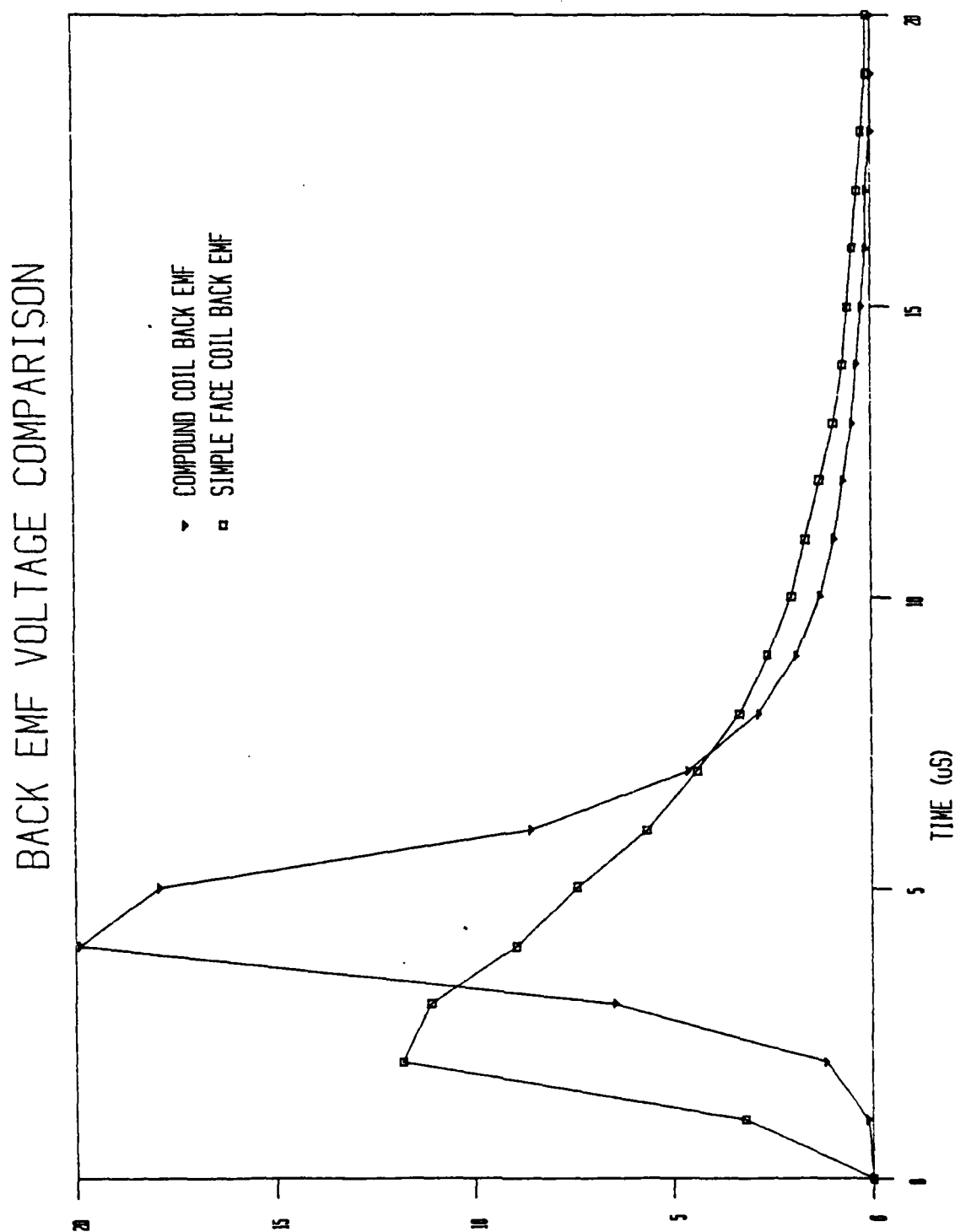
$$\eta = M_{pd}^2 / L_p L_d$$

where  $M_{pd}$  is the mutual inductance between the reaction mass ring and the drive coil and  $L_p$  and  $L_d$  are the self inductances of the ring and drive coil respectively [Mongeau 1981]. It is apparent from this equation that the mutual inductance is the dominant parameter. However, in virtually all drive coil/projectile ring systems, the mutual inductance of the two coils is closely associated with the self inductances of the coils so that an increase in the mutual inductance does not necessarily result in an increase in the efficiency of the system. When electrodynamic effects are added into this analysis, the relationship between the magnetic coupling parameters and engine performance becomes even more complicated.

A particularly surprising and anti-intuitive result of the computer simulation and experimental tests is the discovery that maximum energy transfer to the projectile ring does not occur when the mutual inductance gradient (and thus the thrust) is maximized at the starting position, as one might expect. Maximum energy transfer occurs when the initial thrust is deliberately kept low. There are two distinct reasons for this.

First, there is the induced back EMF which, as in any electric motor, is proportional to speed. If initial acceleration is too high, the back EMF causes the current induced into the projectile ring to saturate. In other words, back EMF in the projectile ring shows up as secondary impedance in the drive circuit and thus limits the power input to the accelerator. Typically, the back EMF is of the same order of magnitude as the  $L(dI/dt)$  voltage in a high performance drive circuit (see figure 9).

Fig. 9: Back-EMF Comparison.



This back EMF saturation effect can be greatly reduced by using pulse coils shaped to minimize the initial accelerating force on the reaction mass ring during the start of the acceleration process. The most simple of these coils is constructed such that the reaction mass ring rests between two sets of coils that make up the drive coil circuit (see figure 10).

In this position, the reaction mass ring has a high mutual inductance with the drive coil but experiences a very low mutual inductance gradient and thus a low accelerating force (see figure 11). As the reaction mass ring moves away from the center of the drive coil, the mutual inductance gradient initially increases and then decreases as the coils move apart. The net result is that more electrical energy can be delivered to the system and converted into kinetic energy.

A second, related effect of high initial thrust is that the projectile moves out of coupling range in a period which is shorter than the rise-time of the accelerating pulse. This decoupling effect simulates high impedance in the drive circuit, and also reduces the amount of energy which is transferred.

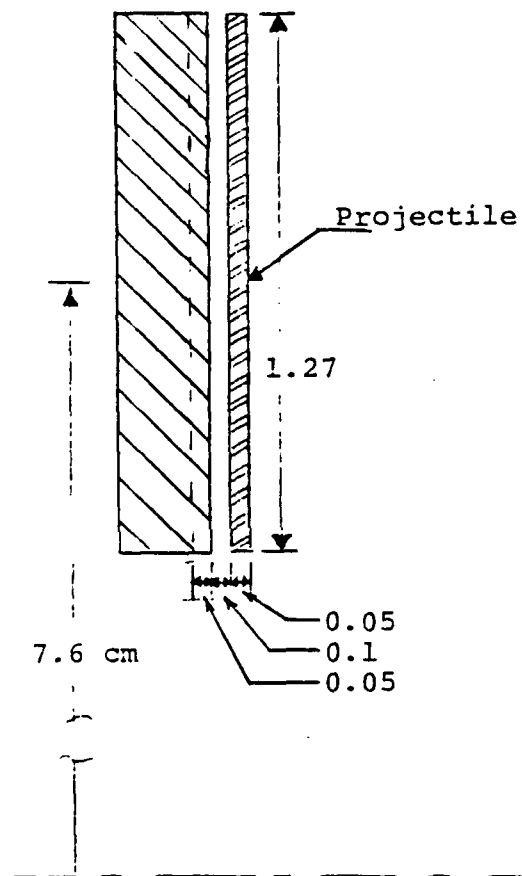
Reducing the initial acceleration thus increases energy transfer by permitting more energy to be stored magnetically in the projectile ring before the ring acquires hypervelocity.

The ideal mutual inductance profile has a maximum near the starting position, and its ideal gradient has a minimum near the starting position.



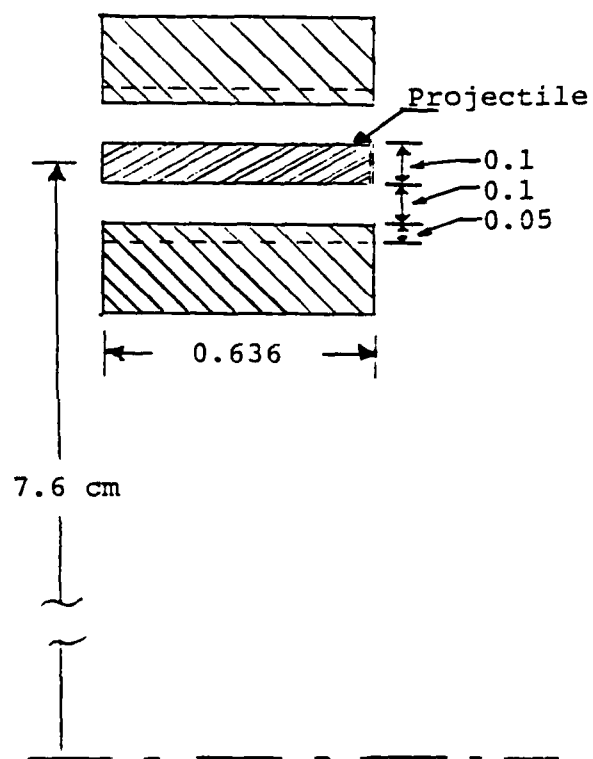
Fig. 10: Simple Face Coil and Compound Coil.

Simple Face Coil



Drive Coil Inductance : 0.317 uH  
Projectile Inductance : 0.325 uH

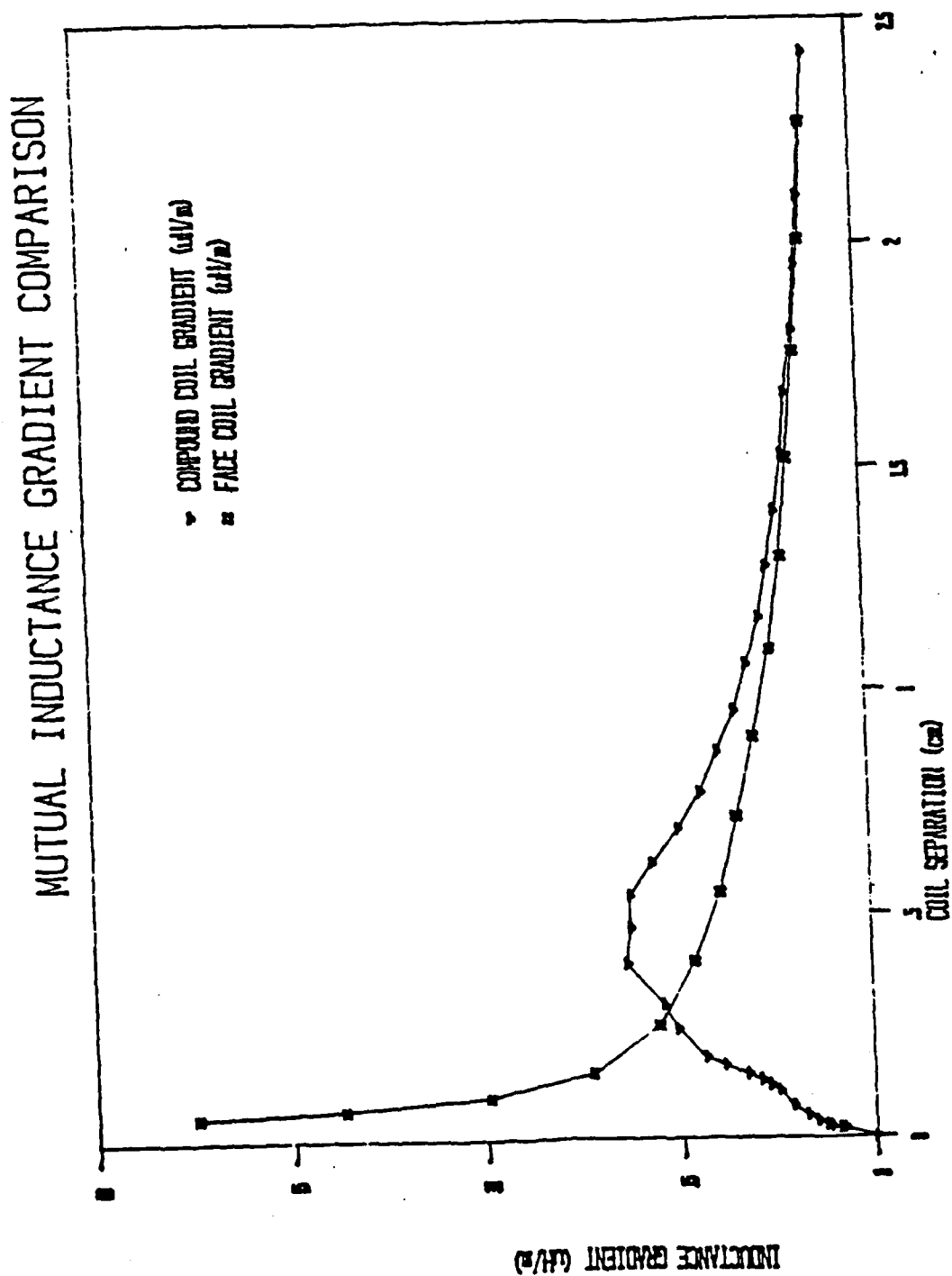
Compound Coil



Drive Coil Inductance : 0.343 uH  
Projectile Inductance : 0.374 uH

Projectile Mass : 8.25 gm

Fig. 11: Mutual Inductance Comparison.



Because the back EMF parameter is so dominant, drive circuit voltages of tens of kilovolts must be used to obtain very high kinetic energy outputs. However, the tremendous thrust developed by this type of accelerator and the close magnetic coupling needed for efficient operation limits the accelerator's performance to the maximum energy that can be handled by the pulse coil.

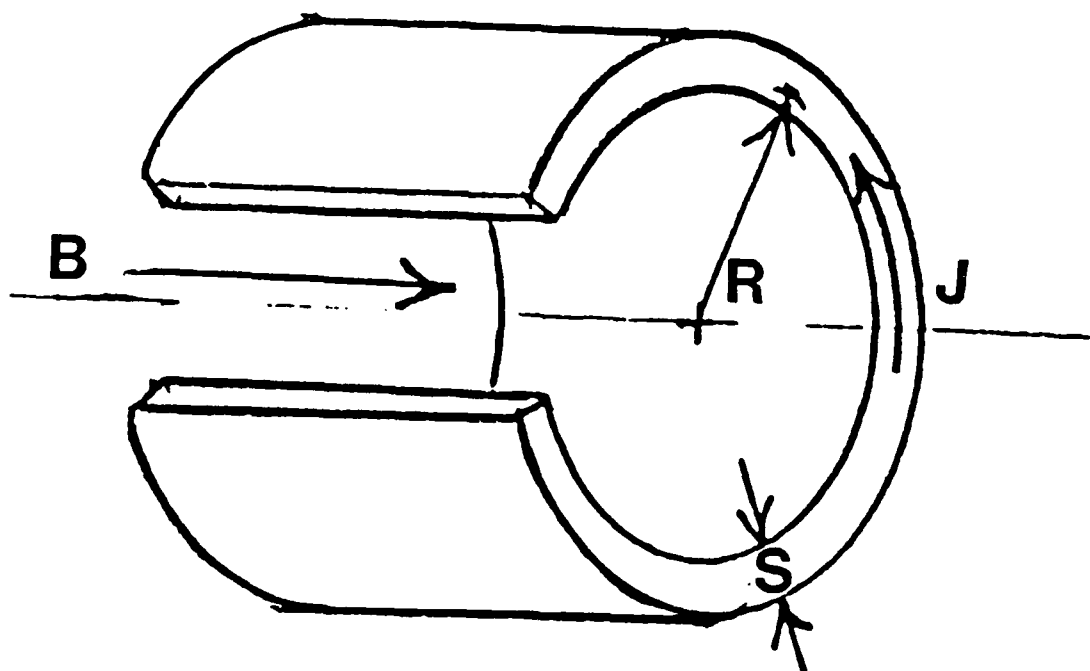
### **PULSE COIL DESIGN**

A given projectile coil is limited by the structural and electrical integrity of the pulse coil used to accelerate it. Analyzing the mode of failure of these coils is difficult since the damage done is usually extensive. However, in most cases it appears that the large impulsive loads exerted on the coils causes the dielectric material to crack. A hot plasma then forms in this crack and blows the coils apart. To date, we have not been able to achieve magnetic fields much higher than twenty tesla. However, significant progress has been made in understanding the mechanics and dynamics of pulse coil design.

At present, pulse coil design is more of an art than it is a science. Even so, there have been pulse coils built that were capable of generating megagauss fields with radial pressures greater than the pressure at the center of the earth. Most of these coils self destruct, but they demonstrate the order of magnitude at which pulse coils are able to operate if only for a brief period of time. When designing a pulse coil for an inductive accelerator, several factors must be taken into consideration: magnetic coupling between the pulse coil and the projectile ring, self inductance of the coil, dielectric breakdown strength between turns, ohmic heating, and the magnetic forces acting on the coil. The true art of pulse coil designing is finding the optimum balance between these key factors.

As with any high kinetic energy device, containing and directing the accelerating forces are the first and foremost issues. In a pulsed induction accelerator, the forces act on the body of the accelerator rather than the surface and are generated by the interaction of the magnetic field around the coils with the currents in the pulse coil and the projectile ring. These forces can be broken into two components, an axial component which acts in compression on the pulse coil and accelerates the projectile ring, and a radial component which is a parasitic force which generates a hoop stress in the two coils (see figure 12).

Fig. 12: Coil Forces.



Optimally, a pulse coil/projectile ring configuration should develop a strong radial magnetic field while minimizing the axial field. In this way, high accelerating forces can be achieved without the coils bursting from radial stresses. The simplest configuration which falls into this category is the face coil. A face coil is a coil wound in a plane perpendicular to the coil's axis of symmetry. By itself, a face coil develops a very high axial field as well as a radial field (see figures 13,14).

However, when a face coil is closely coupled to another coil, the radial field between the two coils becomes quite large but the axial field drops to near zero. What little axial field remains, tends to compress the coils to a finite radius rather than burst them apart (see figures 15,16).

Fig. 13: Uncompensated radial field.

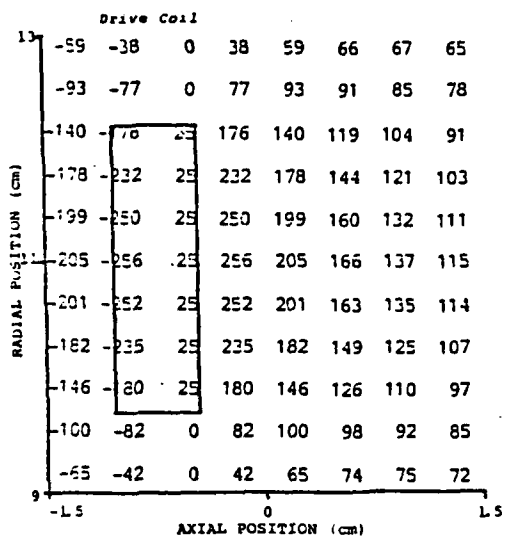


Fig. 14 Uncompensated axial field.

Figure 6. Uncompensated Radial Field Analysis (kG)

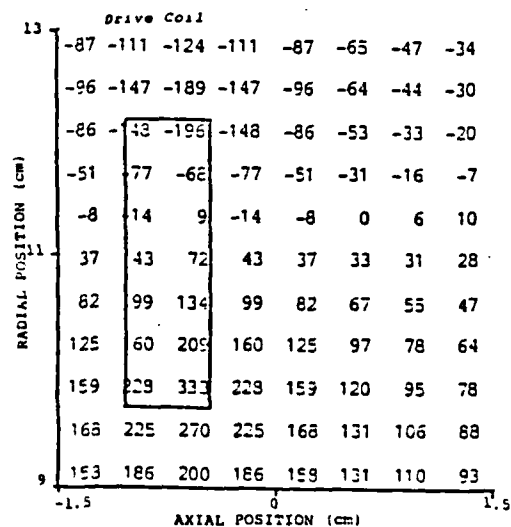


Fig. 15: Compensated radial field.

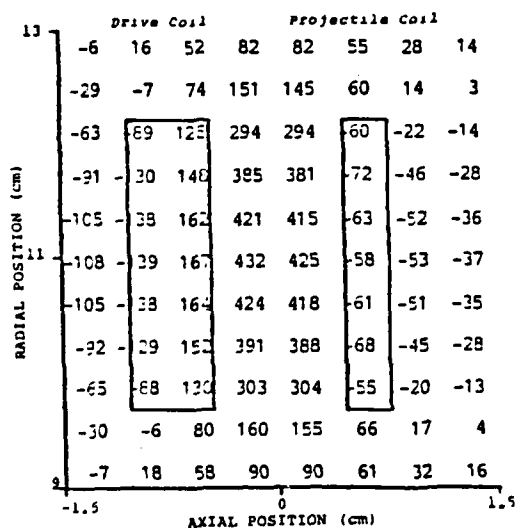


Fig. 16: Compensated axial field.

Figure 8. Compensated Radial Field Analysis (kG)

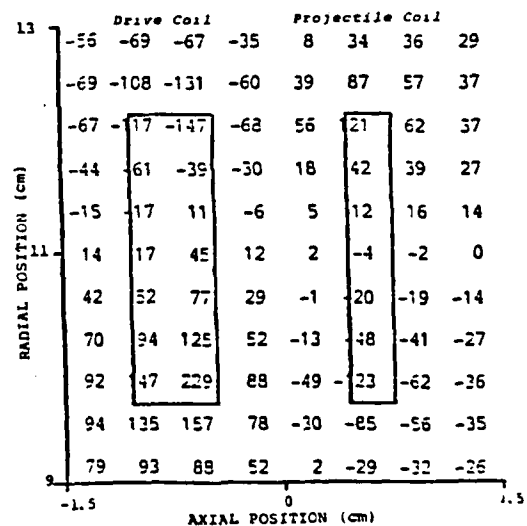


Figure 9. Compensated Axial Field Analysis (kG)

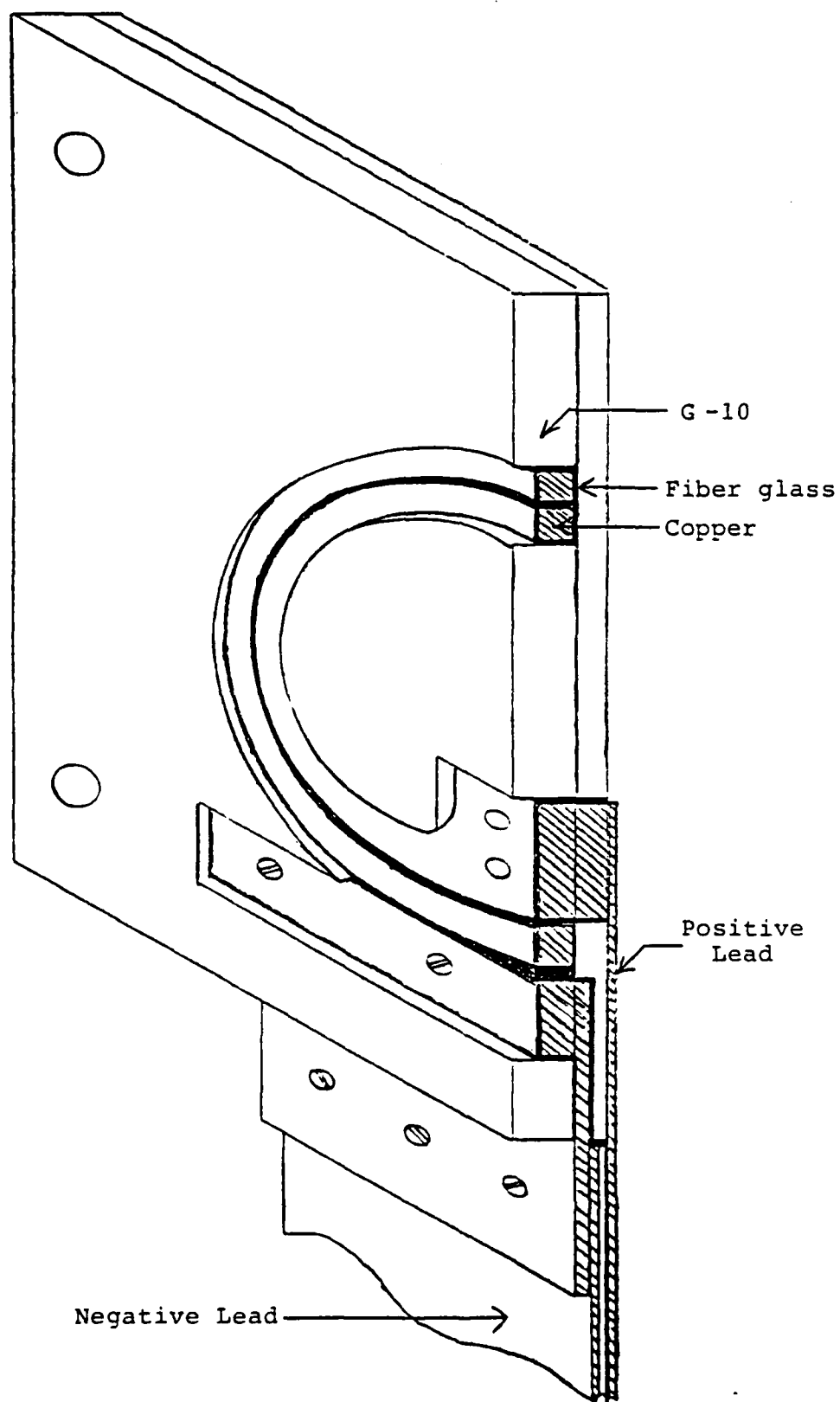
By the time the coils move an appreciable distance from each other and decouple, most of the energy is extracted from the system and the maximum stresses generated are negligible.

Although the bursting force on a pulse coil can be reduced to the point where it is easily contained, the axial force must be taken up by the pulse coil and the structural reinforcement around the pulse coil. This impulsive load can be quite high, on the order of fifty thousand psi, thus making it difficult to contain. In addition to this, there is also the difficulty of providing enough dielectric strength to stand off high voltages between coil turns. These two difficulties are close integral parts of any pulse coil design and it is almost impossible to solve one without influencing the other.

Five different pulse coil designs have been constructed. These coils evolved from a tedious trial and error process in which a coil was design tested to failure and then carefully analyzed. One of the coils constructed was cut from a 1/2" plate of copper, one was formed by winding a 1/2" x 1/16" copper ribbon on edge, and the other three were wound from 1/4" square fiberglass insulated wire. Because of it's structural and electrical properties, G-10 was used in all of these designs as a dielectric material and for structural reinforcement (see figure 17).

The five pulse coil designs were tested in a pulsed induction acceleration apparatus constructed to observe the fundamental mechanisms and limitations of accelerating a projectile coil to hypervelocities. Three of the coils were tested to failure and the other two are still undergoing analysis.

Fig. 17: Typical Coil Design.



### CONCLUSIONS

The pulsed induction acceleration process represents the ultimate interaction between a magnetic field and a metal. It is capable of producing the highest forces and accelerations ever achieved, even in casual experiments using primitive technology. Bandoletov in the USSR accelerated 2 gram rings to one half of earth escape velocity in a launcher length of one inch. These initial results suggest that the process clearly deserves further study because of its scientific interest and potential applications.

We find that the fundamental phenomena and interactions are considerably more subtle than they would seem to be at first sight. Two surprising and anti-intuitive results are that the proximity of a projectile coil tends to reduce the bursting forces on the drive coil, to less than they would be in the absence of a projectile, and that energy transfer to the projectile can actually be increased by deliberately reducing the initial acceleration in the starting position.

We have accelerated 12 gram projectiles to over 700 m/s, at efficiencies above 30 percent. This is comparable to a high-power rifle with a one inch barrel.

In principle it is possible to impart sufficient energy to a projectile ring to cause its melting and evaporation, so that reaction mass in the form of plasma is ejected. In practice, however, the energy transfer is limited by failure of the drive coil in the regime in which melting sets in.

The materials and design of drive coils thus represents a challenge well worth pursuing further.

### ACKNOWLEDGEMENTS

This report represents the second year of a research program to study the basic mechanisms and limitations of the metallic induction reaction engine. The research was performed at Electromagnetic Launch Research, Inc., Cambridge, Massachusetts by Douglas P. Hart, Peter P. Mongeau and Henry H. Kolm. It was supported by the Air Force Office of Scientific Research contract number F49620-84-C-0093. Results of this research were published in thesis form as partial fulfillment of the requirements for the degree of Masters of Science at the Massachusetts Institute of Technology (see final report F49620-83-C-0126.) Summaries have also been submitted for publication in the proceedings of the Electric Propulsion Conference in Alexandria, Virginia and the Pulsed Power Conference in Arlington, Virginia.



#### REFERENCES

Mongeau, P., Coaxial Air Core Electromagnetic Accelerators, Ph.D. Thesis, MIT, October, 1981.

Hart, D., Metallic Induction Reaction Engine, S.M. Thesis, MIT, January, 1985.

Bondaletov, V. N. Ultrahigh Acceleration of Conducting Rings, Soviet Physics Tech. Physl, Vol 22, No. 2, Feb 1977.

**APPENDIX I**

## Experimental and Numerical Performance Comparison

Pulse Coil #1 (3 Turns, 2.85 uH, 1.1 m )

Aluminum Reaction Mass (8.68 grams, 0.33 uH)

| Initial Cap.<br>Voltage | Reaction Ring<br>Velocity (Calc.) | Reaction Ring<br>Velocity (Meas.) | System<br>Efficiency |
|-------------------------|-----------------------------------|-----------------------------------|----------------------|
| 9 kV                    | 495 m/s                           | 498 m/s                           | 29.5 %               |
| 10                      | 565                               | 532                               | 27.3                 |
| 11                      | 635                               | 617                               | 30.3                 |
| 13                      | 776                               | 725                               | 30.0                 |
| 14                      | 847                               | 754                               | 28.0                 |

Pulse Coil #2 (2 turns, 1.4 uH, 0.1 m )

Aluminum Reaction Mass (12.6 grams, 0.28 uH)

|       |         |         |        |
|-------|---------|---------|--------|
| 10 kV | 331 m/s | 365 m/s | 18.7 % |
| 13    | 463     | 440     | 16.0   |

Pulse Coil #3 (4 turns, 2.12 uH, 0.7 m )

Aluminum Reaction Mass (0.7 grams, 0.2 uH)

|      |         |         |       |
|------|---------|---------|-------|
| 7 kV | 451 m/s | 576 m/s | 3.4 % |
| 8    | 493     | 485     | 1.8   |
| 9    | 560     | 640     | 2.5   |

Copper Reaction Mass (2.15 grams, 0.2 uH)

|      |         |         |     |
|------|---------|---------|-----|
| 6 kV | 258 m/s | 207 m/s | 2.8 |
|------|---------|---------|-----|

END

12-86

DTIC